Live Yeast Cell Derivative Induces *c-fos* Expression in THP-1 Monocytes

Andrew Osterburg and Stephen J. Keller*

Department of Biological Sciences, University of Cincinnati, ML 0006, Cincinnati, Ohio, 45221-0006

Abstract: Live Yeast Cell Derivative is a medicinal extract of *Saccharomyces cerevisiae* that has demonstrated efficacy in improving the rate and quality of wound healing in mouse and human systems. However, the mechanisms by which LYCD promotes healing are largely uncharacterized. In this report, we demonstrate that LYCD has effects on the transcriptional profile of the human monocytic cell line THP-1. Thirty minute exposures of THP-1 cells with LYCD induced a 6 to 44-fold, dose-dependent increase in the relative expression of the proto-oncogene c-fos in complete media containing 10% FBS or in low serum media containing 0.1% FBS. Furthermore, protein levels of c-Fos rise at 30 minutes of LYCD exposure and remained detectable for at least 120 minutes of LYCD exposure. However, the relative abundance of the c-fos transcript returned to basal levels by 120 minutes. LYCD also induced expression of c-jun with maximal expression of 3-fold at 60 minutes of exposure. Pretreatments with EGFR kinase inhibitor AG-1478 and the MEK1 inhibitor PD98059 blocked the LYCD-dependent increases in c-fos expression. Consistent with signaling through the EGFR, we have demonstrated by RT-PCR the presence of the mRNA for the EGFR (ErbB1/HER1) in THP-1 cells. Taken together these data suggest that LYCD acts through an EGFR-like cell surface receptor resulting in the activation of the EGFR kinase and the ERK1/2 signaling cascade.

Key Words: THP-1, LYCD, cFos, cJun, EGFR, wound healing.

INTRODUCTION

Live Yeast Cell Derivative (LYCD) is an alcohol extract of stressed stationary phase *Saccharomyces cerevisiae* that has been widely used for over seven decades in over-the-counter medications for relief of hemorrhoidal discomfort. The extract is manufactured under procedures developed by the Sperti Drug Co. (Cincinnati, OH) and appears in commercial products under several different names such as tissue or skin respiratory factor, LYCD, or Biodyne. Topical application of LYCD promotes healing in full thickness excisional wounds made to the backs of the C57BL/KsJ-db/db mouse model of impaired healing. These mice have non-functional leptin receptors, type II diabetes mellitus, and are used extensively as models of impaired wound healing. A histological examination of the LYCD treated wounds suggests that the improved healing occurs at the same time as the infiltration of macrophages and monocytes to the wound [1]. A subsequent study demonstrates that the medicinal activity observed in the C57BL/KsJ-db/db mouse study is the result of a low molecular weight peptide fraction. In addition, the peptide fraction not only improves the rate of healing in C57BL/KsJ-db/db, but also in the excisional wounds of normal C57BL mice [2]. Other investigators show that another low molecular weight protein fraction prepared from LYCD promotes cellular proliferation, collagen synthesis, and angiogenesis in rabbit corneas and chick yolk sacs [3]. A 4.72 kDa protein has been identified in the peptide fraction from LYCD that cross reacts with anti-mouse EGF, and has a dissociation constant of $K_D = 2.26 \pm 0.65$uM to the epidermal growth factor receptor (EGFR) of the human epidermoid carcinoma cell line, A431 [4].

*Address correspondence to this author at the Department of Biological Sciences, 1405 Crosley Tower, University of Cincinnati, Cincinnati, OH 45221-0006, USA; E-mail: kellersj@uc.edu

Wound healing is a complex process involving a diverse set of cell types including keratinocytes, fibroblasts, endothelial cells, and leukocytes. These cells must communicate both spatially and temporally to orchestrate the efficient closure and restoration of damaged tissue. Quick closure of the wound is necessary to prevent the establishment of infections and excessive loss of fluids that may pose a danger to the organism. Therefore diseases with impaired wound healing, such as type II diabetes, represent significant health risks to patients. Treatments that improve the rate of healing may help to reduce medical complications, the economic burden and address the quality of life issues. Experimental evidence demonstrates that under the proper conditions and specific wound requirements, topical application of various exogenous factors such as PDGF-BB, bFGF, TGF-β, EGF, KGF2, and leptin can promote healing [5-8].

Central for the proper progression of healing are monocytes and macrophages [9]. In normal healing, circulating monocytes are recruited, activated, and differentiate into macrophages at the site of injury. Both cells release a cadre of biologically active factors that might serve to regulate other cells within the wound such as keratinocytes and fibroblasts. A recent review discusses the role of inflammatory cells in healing and inflammation [10]. Defects in signaling components that recruit monocytes and macrophages to a wound can delay healing. For example, wounds treated with anti-monocyte inflammatory protein-1alpha (anti-MIP-1α) have fewer macrophages, with a subsequent decrease in angiogenesis and collagen synthesis. In contrast, an overabundunce of macrophage recruitment can lead to chronic inflammation with a delayed onset of healing [11]. However, PU.1 knockout mice, which lack neutrophils and macrophages, can heal wounds without inflammation [12]. These results suggest that cell lineages and cytokines may overlap in their wound healing functions.

1573-4064/08 $55.00+.00

The AP-1 (activator protein-1) transcription factor, composed of homo or heterodimers of Fos (c-Fos, FosB, fra-1, fra-2), Jun (c-Jun, JunB, JunD), ATF and MAF families, is reported to be involved in a wide range of functions in monocytes. For example, AP-1 is involved in the expression of cytokines and growth factors such as: tumor necrosis factor-α (TNFα) [13], interleukin-1β (IL-1β) [14], interleukin-8 [IL-8) [15], and vascular endothelial growth factor (VEGF) [16]. Furthermore, c-*fos* has an important role in modulating macrophage functional activity [17]. Fos and Jun assist in the induction of monocyte differentiation of myeloid cells [18,19].

Despite the *in vivo* effects of LYCD in promoting healing, its effect on inflammatory cells are unknown. Due to the central role of monocytes in healing, we sought to examine the signaling pathways involved and the transcriptional response of cell culture monocytes to LYCD. Additionally, we employed various chemical inhibitors to determine which signaling pathways are involved in LYCD-dependent signaling. THP-1 monocytes are used as a model system to study the effects of medicinal extracts, biomaterials, and other compounds. These cells can be maintained in cell culture, share characteristics with monocytes, exhibit macrophage-like qualities and are used to study monocyte differentiation and maturation [20-23]. Therefore as an amenable model system, we have examined the LYCD-dependent transcriptional response of the AP-1 components *c-fos* and *c-jun*. Alterations in the expression of these genes may reflect changes in the transcriptional state of THP-1 cells to LYCD treatments.

RESULTS

LYCD Induces *c-fos* Expression in THP-1 Cell Culture Monocytes

First we determined if LYCD had any effect on *c-fos* expression in THP-1 cells grown in complete media (RPMI 1640 with 10% FBS). The relative levels for the *c-fos* and *c-jun* transcripts were determined by qPCR using geNorm as described in the methods [24, 25]. For this and subsequent figures the geNorm normalized expression values have been rescaled to the 0 minute or to the vehicle treated samples. The total RNA used in these experiments was quality checked by either MOPS agarose gels or by analysis on an Agilent Bioanalyzer 2100 with RNA sizing microfluidic chips. Only RNA samples with A260/A280 ratios greater than 1.8 and intact 28S and 18S ribosomal bands were used in subsequent analyses. Furthermore, qPCR data was only analyzed if the primers produced bands of the proper size on agarose gels and melting curves produced high temperature melting point peaks.

As can be seen in Fig. (**1**). treatment of THP-1 cell culture with 5 µl/ml of LYCD for 0, 30, 60, 120, and 240 minutes induced the expression of *c-fos*. Maximal expression of *c-fos* occurred 30 minutes after exposure to LYCD resulting in a 12-fold (11.96 ± 3.61) increase over vehicle treated cells. At 60 minutes *c-fos* expression had declined to approximately 5-fold (5.01 ± 2.43) over the 0 minute time point. By 120 minutes of LYCD exposure, *c-fos* mRNA levels had returned to approximately the initial level. Basal levels of *c-fos* expression also were observed at 240 minutes. THP-1 cells maintained in RPMI 1640 with 0.1% FBS for 24 hours prior to experimental treatments had a similar induction of *c-fos* after LYCD treatments (data not shown). The latter experiment suggests that the biologically active portion of LYCD is not competing with a component present in serum. In a set of experiments conducted in RPMI 1640 with 0.1% FBS media, the addition of lipopolysaccharide at 100 ng/ml did not induce *c-fos* after 30 minutes of exposure (Table **1**). This suggests that the THP-1 cells were not responding to LYCD through activation of a non-specific receptor.

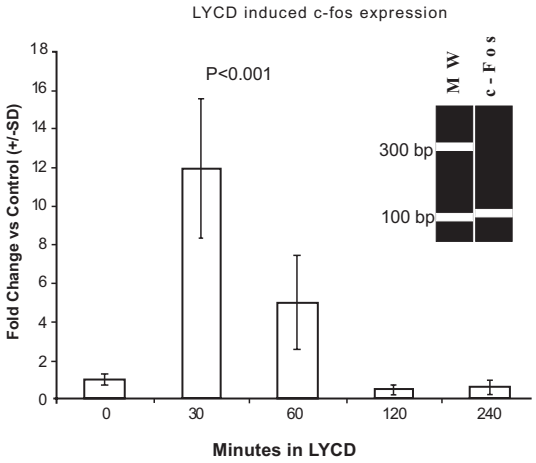

Fig. (1). LYCD induced c-fos expression in THP-1 cells. Cells were grown in RPMI 1640 containing 10% FBS at $5x10^5$ cells/ml for 24 hours prior to treatment with LYCD. Five µl of LYCD was added per ml of media for various times after which total RNA was immediately extracted. Each bar represents triplicate biological samples (n=3) and each qPCR reaction was performed in triplicate. Inset shows false color Agilent Bioanalyzer 2100 analysis of c-fos PCR product.

LYCD Induces *c-fos* in a Dose-Dependent Manner

Next we determined if there was a dose-dependent response of *c-fos* to various LYCD concentrations which might suggest that the response is mediated by a receptor mechanism. We incubated THP-1 cells in low serum media with 20 µl/ml PBS or various doses of LYCD (0.5 µl/ml, 5 µl/ml, 10 µl/ml, and 20 µl/ml) for 30 minutes and measured *c-fos* levels. As can be seen in Fig. (**2**), we observed a dose-dependent response of *c-fos* to LYCD concentrations. Increasing quantities of LYCD resulted in higher fold expression of *c-fos* in relation to the vehicle treated sample. The smallest dose of LYCD (0.5 µl/ml) produced a 6.6-fold increase over the vehicle treated control. Five µl/ml of LYCD resulted in a 20.6-fold induction of the *c-fos* message. At 10 µl/ml of LYCD, there was a 37.9-fold induction of *c-fos*, and at the highest concentration tested (20 µl/ml) we observed a 43.4-fold increase in the relative abundance of *c-fos*. The dose-depen-dent changes of *c-fos* message were found to be highly statistically significant ($P < 0.002$). Furthermore, as the dose of LYCD increased the magnitude of the difference between subsequent doses of *c-fos* decreased. Fitting the normalized expression values for *c-fos* to a linear model re-

Table 1. Effects of the Phosphorylation Inhibitors AG-1478 and PD98059 on c-fos Expression in THP-1 Cells. This table represents various independent experiments in which THP-1 cells were serum starved for 24 hours prior to addition of various inhibitors and LYCD. Vehicle is Ca^{2+}/Mg^{2+} free PBS. All values of c-fos expression have been scaled to their appropriate controls. Pretreatments with DMSO, PD98059, AG-1478, or LPS were for 30 minutes. Each c-fos expression value represents 2 or 3 biological replicates. Relative expression values have been scaled to the appropriate controls. Note a and b are statistically significant versus vehicle treated controls ($P < 0.05$).

Pretreatment	Treatment	c-fos expression	SD
n/a	5µl/ml LYCD[a]	12.77	2.32
DMS0	5µl/ml LYCD[b]	7.61	2.26
10µm AG 1478	5µl/ml LYCD	1.76	0.20
50µm PD98059	5µl/ml LYCD	0.93	0.31
DMSO	vehicle	1.25	0.96
10µm AG 1478	vehicle	1.62	0.36
50µm PD98059	vehicle	1.57	0.74
n/a	100ng/ml LPS	0.91	0.65

sulted in a R^2 of 0.7815 compared to a R^2 of 0.9537 for a fit to a dose-response sigmoidal model. The better fit to a sigmoidal curve is consistent with a receptor based mechanism being involved in mediating LYCD effects.

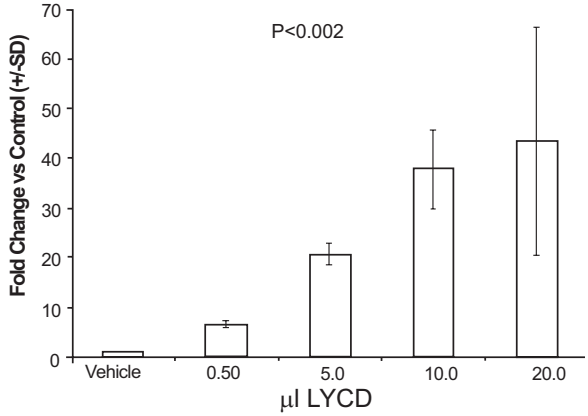

Fig. (2). c-fos expression in serum starved THP-1 cells after 30 minutes with various concentration of LYCD. Cells were grown in RPMI 1640 containing 0.1% FBS at $5x10^5$ cells/ml for 24 hours prior to LYCD treatments. Cells were treated with the given LYCD concentrations for 30 minutes. Total RNA was extracted and qPCR performed. Each bar repre-sents duplicate biological samples (n=2) and qPCR technical replicates (n=3) for each RT reaction.

Exposure of LYCD to THP-1 Cell Cultures Increases *c-jun* Expression

Next we determined the LYCD-dependent changes in *c-jun* expression, a member of the AP-1 transcription factor. Changes in expression were measured after incubation with LYCD for 0, 30, 60, 120, and 240 minutes as presented in (Fig. **3**). By 30 minutes after LYCD treatment of THP-1 cells, the relative abundance of *c-jun* levels had increased 2.5 fold over the 0 minute sample. Maximal expression of *c-jun* was 3-fold and occurred at 60 minutes after addition of LYCD to culture media. By 120 and 240 minutes the levels of *c-jun* had returned to near basal levels. Increased expression of *c-jun* was statistically significant ($P < 0.001$). The expression of *c-fos* and *c-jun* has staggered maxima at 30 and 60 minutes respectively. Additionally, the overall magnitude of the relative increase of these two members of the AP-1 transcription factor was significantly smaller for *c-jun* (3 fold) compared to *c-fos* (12 fold).

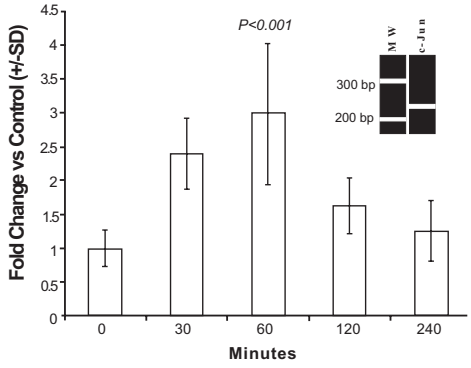

Fig. (3). LYCD induced c-jun expression in THP-1 cells. Cells were grown in RPMI 1640 containing 0.1% FBS at $5x10^5$ cells/ml for 24 hours prior to treatment with LYCD. Five µl of LYCD was added per ml of media for various times after which total RNA was immediately extracted. Each bar represents triplicate biological samples (n=3) and each qPCR reaction was performed in triplicate. Inset shows false color Agilent Bioanalyzer 2100 analysis of c-jun PCR product.

The Phosphorylation Inhibitor (AG-1478) of the EGFR Receptor Kinase Blocks *c-fos* Induction in THP-1 Cells after Exposure to LYCD

Previous work with LYCD has suggested that an epidermal growth factor receptor might be involved in the LYCD

signaling pathway [26]. To determine if this was a potential mechanism for the LYCD-dependent response in THP-1 monocytes, we used the specific EGFR kinase inhibitor AG-1478 to block signaling through the EGFR kinase. This compound has been reported to be highly specific for EGFR kinase and to a lesser degree to ErbB2 kinase [27]. As can be seen in Table **1**, pretreatment of THP-1 cells with 10 μM AG-1478 for 30 minutes prior to the addition of LYCD, resulted in the relative expression of *c-fos* near basal levels (1.76 ± 0.20). Also AG-1478 pretreatment followed by the PBS vehicle for 30 minutes resulted in near basal levels of *c-fos* expression (1.62 ± 0.36). Finally, DMSO pretreatment followed by vehicle showed little increase in *c-fos* levels (1.25 ± 0.96). LYCD treatment in this experiment resulted in a 12.77 ± 2.32 fold increase over the PBS treated control ($P < 0.05$).

The Phosphorylation Inhibitor (PD98059) of ERK1/2 Blocks *c-fos* Induction in THP- 1 Cells after Exposure to LYCD

Next we undertook to determine if the ERK1/2 mitogen activated protein kinase signaling pathway was required for LYCD-dependent *c-fos* expression. We used the MEK1 inhibitor PD98059 to block phosphorylation of ERK1/2. This compound selectively prevents MEK1 phosphorylation of ERK1/2. After 30 minutes. pretreatment with 50 μM PD98059, there was no increase in the relative level of *c-fos* (0.93 ± 0.31) as can be seen in Table **1**. PD98059 followed by vehicle resulted in little induction of the *c-fos* transcript (1.57 ± 0.74). The near basal levels of *c-fos* after AG-1478 and PD98059 inhibition are in contrast to LYCD and DMSO followed by LYCD treatments, in which *c-fos* increases 12.77 ± 2.32 and 7.61 ± 2.26 respectively. Additionally, *c-fos* expression in these latter two treatments is statistically significant ($P < 0.05$) compared to the appropriate vehicle treated controls.

EGFR mRNA is Present in THP-1 Cells

Due to the inhibition of *c-fos* by AG-1478 and PD98059, we sought to determine if mRNAs for any of the four known EGFR isoforms (ErbB1/HER1-ErbB4/HER4) were present in the THP-1 cell line. Total RNA from previous experiments was reverse transcribed using gene specific primers (ErbB1/HER1-ErbB4/HER4) for first strand synthesis. In Fig. (**4A**), RT-PCR was performed with the ErbB1 (EGFR/HER1) primers for two time points (0 min and 240 min) and with biological replicates (A and B) for each time point. This resulted in a PCR product of the predicted size (106 bp) for the EGFR (ErbB1/HER1) primers. To determine if any of the other isoforms (ErbB2/HER2-ErbB4/HER4) were present in these cells a similar set of RT-PCRs were performed using the various ErbB2-4 primers for first strand synthesis. Two biological replicates were used for each isoform (0 min and 240 min). No PCR products were observed for the ErbB2,3,4 isoforms when RT-PCR reactions were analyzed on an Agilent Bioanalyzer 2100 with DNA 1000 microfluidic chips as seen in Fig. (**4B**). To confirm that the primers could amplify the specified products for ErbB2, ErbB3, ErbB4 of the predicted size, 149, 85 and 74 bp respectively, RT-PCR reactions were performed using total RNA from A431 cells. Fig. (**4C**) demonstrates that the gene specific primers produce products of the predicted sizes from A431 total RNA. Only non-specific amplification bands were observed in the cDNA less PCR controls.

LYCD Induced *c-fos* Expression Corresponds to Increased c-Fos Protein Expression

To determine if an increase in the *c-fos* message corresponded to increases in the levels of c-Fos protein, Western blots of protein extracts from LYCD treated THP-1 cells were performed. Cells were treated with 5 μl/ml of LYCD for 0, 30, 60, 120, and 270 minutes. At 0 minutes c-Fos protein levels are below the limit of detection of the chemiluminescence. As can be seen in Fig. (**5**) after 30 minutes of LYCD exposure, we see an approximate 62 kDa band corresponding to c-Fos. There is a decline in band intensity from the 60 minute time point to 270 minutes of LYCD exposure. Blots were stripped and probed for actin as a loading control to ensure that equal quantities of protein were loaded per lane. The background corrected pixel densities for the c-Fos bands were 0, 22212, 20009, 11796, and 0 for 0, 20, 60, 120, and 270 minutes respectively. The background corrected pixel densities for β-actin were 59333, 74723, 73304, 72535, and 66692 for the same time course.

DISCUSSION

LYCD induces *c-fos* expression after treatment of THP-1 monocytes in a time and dose-dependent fashion (Figs. **1, 2**). Maximal transcriptional expression occurred at 30 and 60 minutes for *c-fos* (Fig. **1**) and *c-jun* (Fig. **3**), respectively. This response is consistent with these genes behaving as immediate early genes [28]. The increase in *c-fos* and *c-jun* transcription can alter the composition of the homo- and heterodimers within the AP-1 complex and alter the regulation of target genes [29]. We also measured increased levels of c-Fos protein (Fig. **5**) as a consequence of the increased transcription.

In monocytes and macrophages AP-1 activity is involved in inflammatory and stress related responses. For example, hydrogen peroxide (H_2O_2) produced during respiratory burst activity in macrophages increases the expression of AP-1 and NF-κB [30]. LYCD is reported to contain superoxide dismutase, so it may generate H_2O_2 when added to cells [2]. The respiratory burst activity also activates JNK and ERK1/2 signaling. This link between the redox state of the cell, transcription factors, and signaling pathways can profoundly modulate gene expression. For example, alveolar macrophages upregulate AP-1 in response to acute lung injury [31], increased AP-1 helps protect macrophages from stress induced apoptosis [32], and AP-1 levels are associated with macrophage activation in response to LPS or IFNγ [33]. The AP-1 dimers bind a DNA consensus sequence (TRE response site) which is found in the promoters of genes responsible for cytokines, growth factors, cellular proliferation, differentiation, angiogenesis and apoptosis. We have observed increased transcription of growth factor genes containing containing AP-1 TRE sites in response to LYCD treatments (in preparation).

The data presented in this paper suggests that LYCD induced transcription is dependent upon epidermal growth factor receptor (EGFR) kinase activity. We have demon-

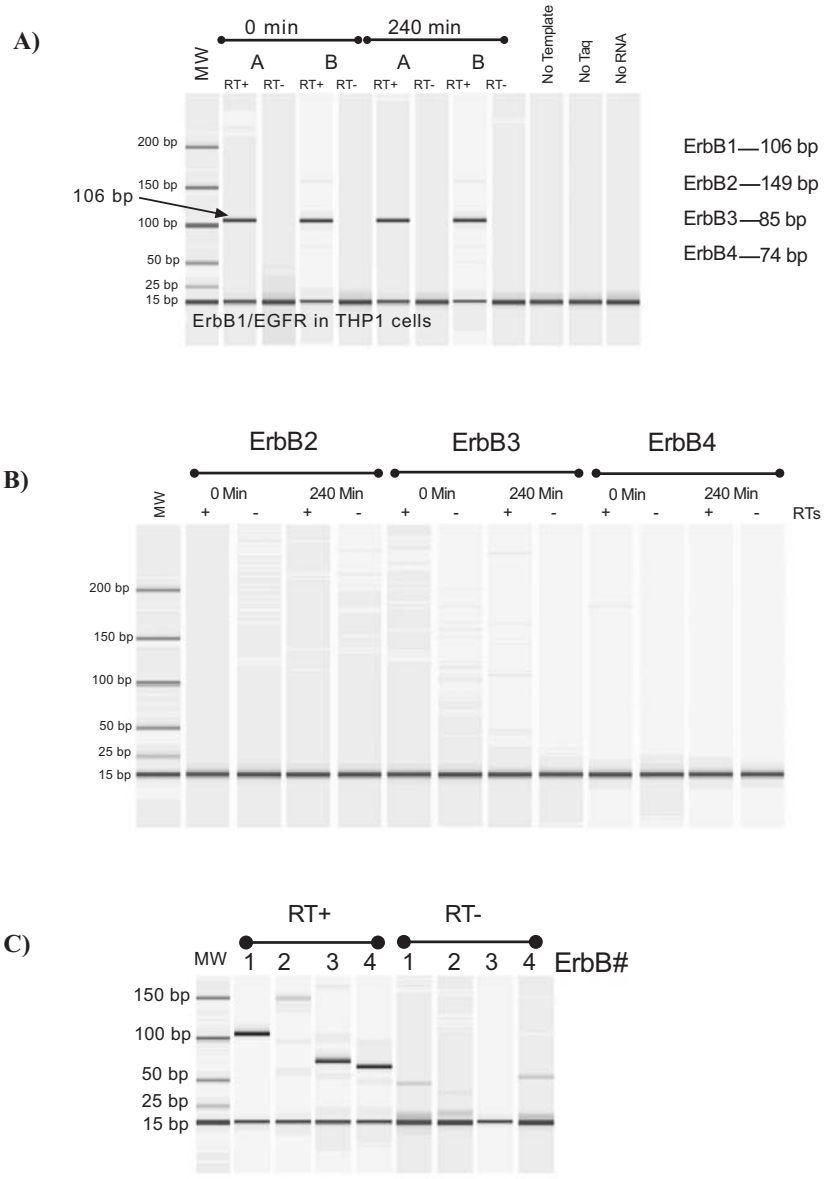

Fig. (4). RT-PCR of THP-1 total RNA for ErbB isoforms. Total RNA from LYCD treated THP-1 cells was used to detect the presence of the ErbB isoforms. A) Two biological replicates (A and B) were used from 2 time points (0 min, and 240 min). PCR products were separated and analyzed using a Agilent bioanalyzer 2100 DNA sizing microfluidic chip. B) RT-PCRs for ErbB2 thru ErbB4 in THP1 cells. Each RT for each isoform was run in biological duplicate (0 min and 240 minutes). The +/- represent the presence/absense of the reverse transcriptase in the reaction. C) Positive controls for the primers using total RNA extracted from A431 cells. The band at 15 bp represents a sizing marker present in each lane.

strated the presence of the EGFR message in THP-1 cells, as well as the inhibition of *c-fos* induction after inhibition of EGFR kinase activity by AG-1478 (Table **1**). Until recently, the evidence for the EGFR on monocytes and macrophages was scant. However microglia cells, descendents of the myeloid lineage as well as the U937 monocyte cell line are reported to express the EGFR [34,35]. The EGFR was functional in the U937 cell line since researchers found that an activating antibody (ICR9) increased the rate of proliferation. Furthermore, at low concentrations, the ICR62 antibody, which blocks the EGF binding pocket on the EGFR, reduced levels of U937 proliferation. Lamb and coworkers have also shown the presence of the EGFR on peripheral blood monocytes and macrophages [36]. This EGFR appears to be functional since it mediates chemotaxis in monocytes and macrophages and cellular proliferation of macrophages. In atherosclerotic plaques, EGFR co-localized with the macrophage marker RAM11 which suggests a receptor role specifically in atherogenesis and generally in chronic inflammation. Therefore, the expression of the EGFR on

monocytes and macrophages may be a product of inflammation and potentially contributes to monocyte / macrophage chemotaxis and proliferation in wounds.

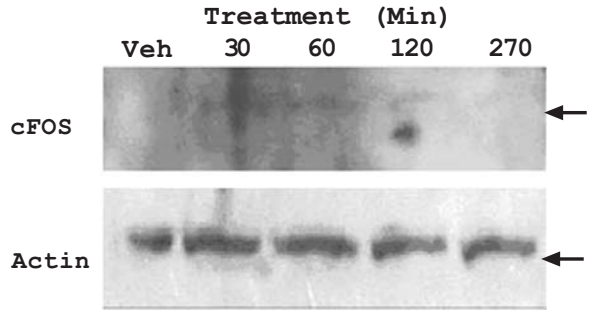

Fig. (5). Western blot of cFos from LYCD treated THP-1 cells. Cells were grown in RPMI 1640 containing 0.1% FBS at $5x10^5$ cells/ml for 24 hours prior to treatment with LYCD. Five µl of LYCD was added per ml of media for various times after which a protein lysate was prepared (Methods). The time of LYCD exposure is given above each lane. A non-LYCD control is in the first lane. After cFos detection, the blot was stripped and the amount of β-actin in each lane was used as a loading control.

The current set of experiments, LYCD-dependent *c-fos* induction, inhibition by AG-1478 and PD98059 (Table **1**), and the demonstration of the EGFR message (Fig. **4**) are all consistent with LYCD signaling through the EGFR in THP-1 monocytes. The data presented here is the first report that the EGFR mRNA is present in THP-1 monocytes. This is in contrast to Mograbi *et al*. who did not detect EGFR message by RT-PCR in phorbol 12, 13-dibutyrate (PDBu) treated THP-1 cells [37]. One explanation for this discrepancy may be that there is an alternatively spliced form of the EGFR present in the THP-1 cell line. The primers that Mograbi *et al*. used spanned exons 1-23 whereas the primers used here spanned exon 26-27. These latter primers correspond to the intracellular kinase domain of the receptor. If there is an alternatively spliced form of the receptor, the forward primer used by Mograbi *et al*. may not have had a target sequence. For example, the kinase region of the EGFR is present in a number of mutant forms of the EGFR but exon 1 has been shown to be absent in at least one mutant (EGFRvI) [38]. These EGFR mutants have been associated with various tumors. However, due to the observed *in vivo* effects of LYCD induced healing in *db/db* mice, and in human skin graft donor sites, we feel that a tumor-associated mutant form of the receptor mediating LYCD signaling is unlikely.

The EGFR mediates signaling events that extend beyond the EGF-specific ligand activation. For example, the platelet derived growth factor receptor has been shown to heterodimerize with EGFR [39]. Additionally, stimulation of G-protein coupled receptors can activate EGFR tyrosine kinase signaling. Signaling by the EGFR then occurs through classical intracellular signaling cascades [40]. A transactivating mechanism, or noncanonical EGFR partner, for LYCD-dependent EGFR signaling remains a possibility in THP-1 cells especially since LYCD can generate H_2O_2, a known EGFR transactivator [41].

There are alternate explanations for AG-1478 blocking LYCD-dependent induction of *c-fos*. AG-1478 has recently been reported to have broader inhibitory effects than initially reported. These other targets could potentially account for the LYCD-dependent transcriptional changes of *c-fos* in our system. For example, AG-1478 has been shown to specifically bind to and block the Kv1.5 potassium voltage channel (Kv1.5) in a non-PTK dependent manner in Chinese hamster ovary cells (CHO) [42]. However, this effect does not account for the inhibition of *c-fos* by the MEK1 inhibitor PD98059. Recently, it was shown that in $Kv1.3^{-/-}$ mice there was suppression of c-Jun N-terminal kinase (JNK) activation [43]. Although the mechanism of this suppression was not described, it suggests that there are potential links between potassium voltage channels and MAPK pathways which could provide an explanation for both AG-1478 and PD98059 inhibition of *c-fos* expression. The identity of the LYCD receptor currently remains unknown. Our data suggests that the receptor which mediates the LYCD response possesses 'EGFR-like' qualities.

In conclusion, we have shown a potential role for LYCD in regulating monocyte function through modulation of *c-fos* and *c-jun* levels. LYCD contains two peptides that are candidates for the signal: (1) a 4.7 kDa peptide which binds EGFR [4] and (2) superoxide dismutase [2] that produces H_2O_2, a transactivator of the EGFR. Changes in the abundance of these transcripts suggests that AP-1 DNA binding and subsequent downstream effects of THP-1 monocytes is being modulated by LYCD. This transcription factor has been implicated in wound regeneration in keratinocytes and appears to play a role in monocyte signaling and inflammatory responses. Transcriptional targets of the altered subunit composition of AP-1 due to LYCD exposure may help to explain the observed effects of LYCD in promoting wound healing. Additional data to be published is consistent with this interpretation since cell cycle, growth factor, apoptotic, and oxidative stress related genes have altered expression in response to LYCD exposure. We have shown that LYCD treated monocytes have altered cytokine and growth factor profiles in response to LYCD [44]. Therefore, the increase in transcription of c-Fos/c-Jun may represent increased binding to AP-1 TRE binding sites which serve to enhance the AP-1 dependent transcription in THP-1 monocytes. Furthermore, AP-1 binding may modulate the monocyte and macrophage phenotype in LYCD treated cells to one that promotes healing. Components of the LYCD preparation may prove to be a cost effective and a safe treatment for the promotion of healing in impaired wounds.

MATERIALS AND METHODS

Reagents

LYCD was provided by the Lotus Group, Inc. (Cincinnati, OH) with a certificate of analysis demonstrating the extract was sterile and stimulated the respiration of A431 human epidermoid carcinoma cells. The preparation was supplied as an aqueous solution in calcium and magnesium free phosphate buffered saline (PBS) at a protein concentration of 15 mg/ml. All primers were purchased from Integrated DNA Technologies (Coralville, IA). AG-1478 [4-(3-Chloroanilino)-6,7-dimethoxy quinazoline] and PD98059

[2′-Amino-3′-methoxyflavone] were purchased from EMD Biosciences (San Diego, CA). Lipopolysaccharide from *E.coli* 026:B6 (LPS) was purchased from Sigma-Aldrich Corp. (St. Louis, MO).

Cell Culture

THP-1 cells were obtained from ATCC (American Type Culture Collection, Manassas, VA). The cells were maintained in 5% CO_2 at 37˚C between $5x10^4$ and $8x10^5$ cells/ml in RPMI 1640 supplemented with 2 mM L-glutamine, 1.5 g/L sodium bicarbonate, 4.5 g/L glucose, 10 mM HEPES, 1.0 mM sodium pyruvate, 0.05 mM 2-mercaptoethanol, and 10% heat inactivated fetal bovine serum (Invitrogen, Carlsbad, CA). For each experiment, the cells were counted in a standard hemocytometer and resuspended at $5x10^5$ cells/ml in either RPMI media containing 10% heat inactivated fetal bovine serum (FBS) or in low serum RPMI media containing 0.1% FBS for 24 hours prior to the experimental treatments.

A431 human epidermoid carcinoma cells were obtained from ATCC. The cells are grown in Dulbecco's Modified Eagle's Medium, (DMEM) supplemented with 1.5 g/L sodium bicarbonate, 10 mM HEPES, and 10% fetal bovine serum (Invitrogen) at 37°C in 5% CO_2.

RNA Isolation for Real-time qPCR

Total RNA from THP-1 cells was isolated using TRI Reagent (Molecular Research Center, Cincinnati, OH) according to the manufacturer's protocol with one additional 75% ethanol wash. Briefly, the cells were centrifuged at 300g for 3 minutes (min.). One ml of TRI reagent was added to disrupt the cells and the samples were vigorously mixed and incubated at room temperature for 15 min. One hundred µl of 1-bromo-3-chloropropane (BCP) was added and each sample was centrifuged at 12,000g for 15 min. at 4ºC. The RNA containing aqueous layer was removed and mixed with 0.5 ml of 100% isopropanol. After 5 min., the samples were centrifuged at 12,000g for 15 min. at 4ºC and the pellet washed two times with 1 ml of 75% ethanol. After the final wash the supernatant was discarded and the pellets were air dried for 5-10 min. RNA was resuspended in 15-20 µl of RNase/DNase free water and incubated at 37˚C for 15 min. Residual genomic DNA contamination was removed with DNA-*free* (Ambion Inc., Austin, TX) according to the manufacturer's protocol. Briefly, 0.1 volumes of 10X DNase I buffer and 1 µl of DNase I was added to each RNA sample. After 30 min. incubation at 37ºC, 0.1 volume of the DNase Inactivation Agent was added to each tube. The samples were incubated for 2 min. at room temperature, centrifuged for 2 min. at 12,000g and the supernatants were transferred to new tubes for subsequent analysis. Spectrophotometric quantification of RNA was performed on a Shimadzu UV-VIS Spectrophotometer (Shimadzu Scientific Instruments, Inc., Columbia, MD). The RNA was stored at -80ºC until needed for the reverse transcription (RT) reactions. RNA integrity was determined by comparing the 28S and 18S bands on either formaldehyde/MOPS gels or by use of an Agilent Bioanalyzer 2100 (Agilent Technologies, Palo Alto, CA) with RNA 6000 Nano LabChip micro-fluidic chips according to the manufacturer's recommendations.

Reverse Transcription (RT) for qPCR

Two µg of total RNA from each biological replicate were reverse transcribed using SuperScript II (Invitrogen, Carlsbad, CA) and the first strand primer Oligo-$d(T)_{23}$VN (where V= A, G, C, and N= A, T, C, G) (New England Biolabs, Ipswich, MA). The first strand thermal conditions were: 25°C for 10 min., followed by 42°C for 30 min., and finally 70˚C 15 min. as recommended by the manufacturer. RNase inhibitor and the dNTP Mix were purchased from Applied Biosystems (Foster City, CA). After cDNA synthesis, RT reactions were diluted 1:5 in double distilled RNase free, DNase free water for use in the qPCR reactions.

To determine if the EGFR and HER2, HER3, and HER4 mRNA were present in THP1 cells, we used the Clontech Advantage RT-for-PCR kit according to the manufacturer's protocol (Clontech, Mountain View, CA). The first strand was synthesized with the appropriate gene specific primers. Positive controls for the reaction were total RNA isolated from human epidermoid carcinoma A431 cells that have been shown to express all four forms of the ErbB/HER family [45].

Primers

The *c-fos* and *c-jun* primers were designed with the aid of the Primer3 website (http://frodo. wi.mit.edu/cgi-bin/primer3/primer3_www.cgi) from the NCBI files NM_005252 and NM_002228 respectively. Sequences for normalization with geNorm were obtained from Vandesompele *et al*. [24]. The sequences for identification of the EGFR mRNA and its isoforms were taken from Bieche *et al*. [46]. *c-fos* Forward, 5'-ACTGCTTACACGTCTTCCTTCGTC-3', *c-fos* Reverse 5'-TTCTCCTCTCTGTAATGCACCAGC-3', 213 bp; *erbB1/HER1* Forward 5'-GGTGTGTGCAGATCGCAAAG-3', *erbB1*/*HER1* Reverse 5'-GACATGCTGCGGTGTTTTCAC-3', 106 bp; *erbB2*/*HER2* Forward 5'-AGCCGCGAGCACC-CAAGT-3', *erbB2*/ *HER2* Reverse 5'-TTGGTGGGCAGGT-AGGTGAGTT-3', 147 bp; *erbB3*/*HER3* Forward 5'-GT-CTGTGTGACCCACTGCAACT-3', *erbB3*/*HER3* Reverse 5'-GGGTGGCAGGAGAAGCATT-3', 80 bp; *erbB4*/*HER4* Forward 5'-GGCTGCTGAGTTTTCAAGGATG-3', *erbB4*/*HER4* Reverse 5'-GCTTCATACGATCATCACCCTGA-3', 74 bp; *c-jun* Forward 5'-TGGAAACGACCTTCTATGA CGA-3', *c-jun* Reverse 5'-GTTGCTGGACTGGATTAT-CAGG-3', 241 bp. All primers produced products of the expected size when PCR products were checked by agarose gel electrophoreses or on the Agilent 2100 Bioanalyzer. Additionally, melting curves were examined on the final PCR products to ensure that only the appropriate amplicons were produced in the reaction.

Real-time Quantitative PCR (qPCR)

Real-time quantitative PCR (qPCR) was performed using the DyNAmo SYBR Green qPCR 2X Master mix (Bio-Rad Laboratories, Hercules, CA) in 96-well plates (Bio-Rad). The total reaction volumes were 20 µl per reaction, with 0.4 µM of the appropriate primers and 2 µl of a 1:5 dilution of the reverse transcription reaction. After the addition of the all reagents, the plates were sealed with Microseal 'B' Seal (Bio-Rad). Thermal cycling was performed in a MJ Opticon 2 (Bio-Rad) and the Ct values and melting curves were deter-

mined with the Opticon2 (ver 2.02) software. Cycling conditions were: 95ºC for 15 min., followed by 40 cycles of 95ºC for 10 sec, 60ºC for 20 sec, and 72ºC for 20 seconds. After each extension cycle, the SYBR green fluorescence was measured.

Data Normalization

GeNorm was used to find the most stable housekeeping genes (HKG) for normalization of qPCR expression data [24]. The most stable set of HKGs were determined by measuring all of the relative pairwise expression values of a panel of housekeeping genes by the comparative Ct method. The most stable set of HKGs over all of the time points and treatments were determined to be: β-actin (ACTB), hypoxanthine phosphoribosyl transferase (HPRT), glyceraldehyde-3-phosphate dehydrogenase (GAPDH), and β-2-microglobulin (B2M). This set of HKGs had a stability measure (M) of 0.201. From this set of genes, normalization factors were derived from the geometric mean of their relative expression from each RT reaction. Additionally, the average efficiencies of amplification for each gene were used by measuring per-well efficiencies with LinRegPCR [25]. Each experiment had 2 or 3 biological replicates per treatment and each qPCR reaction had 3 technical replicates.

Statistics

Differences between expression levels were taken to be statistically significant at $P < 0.05$. To determine the statistical significance for qPCR data, the Resampling Stats (Arlington, VA) software package was used [47]. Resampling Stats was used to calculate a distribution of possible F-ratios from the geNorm normalized expression values from biological replicates. The reported *P*-value was determined from the frequency of the observed F-ratio in the hypothetical F-ratio distribution calculated by Resampling Stats.

Western Blot Analysis

Antibodies for c-Fos (H-125, a polyclonal rabbit IgG) , β-actin (C-11, a polyclonal goat IgG), horseradish peroxidase (HRP) conjugated secondary antibodies (bovine anti-rabbit IgG, and rabbit anti-goat IgG) were purchased from Santa Cruz Biotechnology, Inc (Santa Cruz, CA).

THP-1 cells were suspended at $5x10^5$ cells/ml in low serum RPMI 1640 for 24 hours prior to the experiments. After various LYCD treatments, the cells were washed with ice cold PBS and collected at 300g for 5 min. Proteins were extracted with M-PER (Mammalian Protein Extraction Agent, Pierce, Rockford, IL) according to the manufacturer's recommendations. Protein quantification was performed with the Bradford reagent at A590 measured on a Molecular Devices 96-well υmax micro-plate reader (Sunnyvale, CA). Twenty μg of protein lysate were loaded per lane on 4% - 20% precast Tris-HCl gels (Bio-Rad) and the gels were run at 20 mA until the dye-front reached the bottom. The gel was equilibrated in Towbin buffer (20% MeOH, 25 mM Tris, 192 mM Glycine) for 30 min. at room temperature, followed by semi-dry electro-transfer to 0.45 μm PVDF membranes (Immobilon-P, Millipore, Bedford, MA) for 1 hour at 100 mA. The membranes were blocked with 1% casein in PBS (Casein PBS Blocking Buffer, Pierce, Rockford, IL) supplemented with molecular biology grade 0.05% Tween-20 for 1 hour at room temperature with shaking. Primary and secondary antibodies were used at 1:100 and 1:5000 dilutions respectively in a modified blocking buffer (0.5% casein blocker with 0.05% Tween-20 in PBS) for 2 hours at room temperature or overnight at 4˚C with shaking. Membranes were washed three times for 10 min. each in TPBS (PBS with 0.05% Tween-20) followed by one wash in PBS. The bound antibodies were visualized using HRP-conjugated secondary antibodies followed by chemiluminescence (ECL-Plus, Amersham Pharmacia, Piscataway, NJ). Kodak XAR Film (Fisher Scientific) was used for chemiluminescent detection.

For visualization of β-actin, the membranes were stripped with glycine stripping buffer (0.2 M glycine, 0.1% SDS, 1% Tween-20, pH 2.2) two times for 30 min. each at room temperature with shaking. Membranes were washed three times in PBS. Membranes were blocked for 1 hour at room temperature with shaking and antibody staining proceeded as described above. Pixel densities were determined using the free object quantification tool, with the boarder subtraction, in GelExpert 3.5 (NucleoTech, San Mateo, CA).

ACKNOWLEDGEMENTS

This work was partially supported by a NIH grant to the Lotus Group and by the University of Cincinnati Research Foundation through the generosity of the Schlemm family.

REFERENCES

[1] Crowe, M.J.; McNeill, R.B.; Schlemm, D.J.; Greenhalgh, D.G.; Keller, S.J. *J. Burn Care Rehabil*., **1999**, *20*, 155.
[2] Schlemm, D.J.; Crowe, M.J.; McNeill, R.B.; Stanley, A.E.; Keller, S.J. *Cell Stress Chaperones*, **1999**, *4*, 171.
[3] Bentley, J.P.; Hunt, T.K.; Weiss, J.B.; Taylor, C.M.; Hanson, A.N.; Davies, G.H.; Halliday, B.J. *Arch. Surg*., **1990**, *125*, 641.
[4] Levin, R.H.; Keller, S.J. Yeast-Derived Epi-dermal Growth Factor. US Patent 5,219,998, Jun 15, 1993.
[5] Robson, M.C. *Wound Rep. Reg.*, **1995**, *5*, 12.
[6] Hong, J.P.; Kim, Y.W.; Jung, H.D.; Jung, K.I. *Int. Wound J.*, **2006**, *3*, 123.
[7] Geer, D.J.; Swartz, D.D.; Andreadis, S.T. *Am. J. Pathol*., **2005**, *167*, 1575.
[8] Ring, B.D.; Scully, S.; Davis, C.R.; Baker, M.B.; Cullen, M.J.; Pelleymounter, M.A.; Danilenko, D. M. *Endocrinology*, **2000**, *141*, 446.
[9] Burke, B.; Lewis, C.E. *The Macrophage*, 2nd ed.; Oxford University Press: New York, **2002**
[10] Martin, P.; Leibovich, S.J. *Trends Cell Biol*., **2005**, *15*, 599.
[11] Graves, D.T.; Kayal, R.A. *Front. Biosci*., **2008**, *13*, 1227.
[12] Martin, P.; D'Souza, D.; Martin, J.; Grose, R.; Cooper, L.; Maki, R.; McKercher, S.R. *Curr. Biol*., **2003**, *13*, 1122.
[13] Krämer, B.; Wiegmann, K.; Krönke, M. *J. Biol. Chem*., **1995**, *270*, 6577.
[14] Kang, J.S.; Yoon, Y.D.; Lee, K.H.; Park, S.K.; Kim, H.M. *Biochem. Biophys. Res. Commun*., **2004**, *313*, 171.
[15] Liu, R.; O'Connell, M.; Johnson, K.; Pritzker, K.; Mackman, N.; Terkeltaub, R. *Arth. Rheum*., **2000**, *43*, 1145.
[16] Tischer, E.; Mitchell, R.; Hartman, T.; Silva, M.; Gospodarowicz, D.; Fiddes, J.C.; Abraham, J.A. *J. Biol. Chem*., **1991**, *266*, 11947.
[17] Collart, M.A.; Belin, D.; Vassalli, J.D.; Vassalli, P. *J. Immunol*., **1987**, *139*, 949.
[18] Müller, R.; Curran, T.; Müller, D.; Guilbert, L. *Nature*, **1985**, *314*, 546.
[19] Friedman, A.D. *Oncogene*, **2007**, *26*, 6816.
[20] Tsuchiya, S.; Yamabe, M.; Yamaguchi, Y.; Kobayashi, Y.; Konno, T.; Tada, K. *Int. J. Cancer*, **1980**, *26*, 171.
[21] Auwerx, J. *Experientia*, **1991**, *47*, 22.

[22] Heil, T.L.; Volkmann, K.R.; Wataha, J.C.; Lockwood, P.E. *J. Oral Rehabil*., **2002**, *29*, 401.
[23] Berges, C.; Naujokat, C.; Tinapp, S.; Wieczorek, H.; Höh, A.; Sadeghi, M.; Opelz, G.; Daniel, V. *Biochem. Biophys. Res. Commun.*, **2005**, *333*, 896.
[24] Vandesompele, J.; De Preter, K.; Pattyn, F.; Poppe, B.; Van Roy, N.; De Paepe, A.; Speleman, F. *Genome Biol*., **2002**, *3*, RESEARCH0034 Epub.
[25] Ramakers, C.; Ruijter, J.M.; Deprez, R.H.; Moorman, A.F. *Neurosci. Lett*. **2003**, *339*, 62.
[26] Fang, J. M.S. Thesis, University of Cincinnati, Cincinnati, OH, **1992**.
[27] Egeblad, M.; Mortensen, O.H.; van Kempen, L.C.L.T.; Jäättelä, M. *Biochem. Biophys. Res. Commun*., **2001**, *281*, 25.
[28] Sng, J.C.; Taniura, H.; Yoneda, Y. *Biol. Pharm. Bull*., **2004**, *27*, 606.
[29] Karin, M.; Liu, Z.; Zandi, E. *Curr. Opin. Cell Biol*., **1997**, *9*, 240.
[30] Iles, K.E.; Forman, H.J. *Immunol. Res*., **2002**, *26*, 95.
[31] Guo, R.F.; Lentsch, A.B.; Sarma, J.V.; Sun, L.; Riedemann, N.C.; McClintock, S.D.; McGuire, S.R.; Van Rooijen, N.; Ward, P.A. *Am. J. Pathol*., **2002**, *161*, 275.
[32] Liebermann, D.A.; Gregory, B.; Hoffman, B. *Int. J. Oncol*., **1998**, *12*, 685.
[33] Higuchi, Y.; Setoguchi, M.; Yoshida, S.; Akizuki, S.; Yamamoto, S. *Oncogene*, **1988**, *2*, 515.
[34] Kalyani, A.J.; Mujtaba, T.; Rao, M.S. *J. Neurobiol*., **1999**, *38*, 207.
[35] Eales-Reynolds, L.J.; Laver, H.; Mojtahedi, H. *Cytokine*, **2001**, *16*, 169.
[36] Lamb, D.J.; Modjtahedi, H.; Plant, N.J.; Ferns, G.A. *Atherosclerosis*, **2004**, *176*, 21.
[37] Mograbi, B.; Rochet, N.; Imbert, V.; Bourget, I.; Bocciardi, R.; Emiliozzi, C.; Rossi, B. *Eur. Cytokine Netw*., **1997**, *8*, 73.
[38] Kuan, C.T.; Wikstrand, C.J.; Bigner, D.D. *Endocr. Relat. Cancer*, **2001**, *8*, 83.
[39] Saito, Y.; Haendeler, J.; Hojo, Y.; Yamamoto, K.; Berk, B.C. *Mol. Cell. Biol*., **2001**, *21*, 6387.
[40] Fischer, O.M.; Hart, S.; Gschwind, A.; Ullrich, A. *Biochem. Soc. Trans*., **2003**, *31*, 1203.
[41] Zhougang, S.; Schnellmann, R.G. *Am. J. Physiol. Renal Physiol.,* **2004**, *286*, F858.
[42] Choi, B.H.; Choi, J.S.; Rhie, D.J.; Yoon, S.H.; Min, D.S.; Jo, Y.H.; Kim, M.S.; Hahn, S.J. *Am. J. Physiol. Cell Physiol*., **2002**, *282*, C1461.
[43] Xu, J.; Wang, P.; Li, Y.; Li, G.; Kaczmarek, L.K.; Wu, Y.; Koni, P.A.; Flavell, R.A.; Desir, G.V. *Proc. Natl. Acad. Sci. USA*, **2004**, *101*, 3112.
[44] Osterburg, A. Ph.D. Thesis, University of Cincinnati, Cincinnati, OH, **2005**.
[45] Stoll, S.W.; Kansra, S.; Peshick, S.; Fry, D.W.; Leopold, W.R.; Wiesen, J.F.; Sibilia, M.; Zhang, T.; Werb, Z.; Derynck, R.; Wagner, E.F.; Elder, J.T. *Neoplasia*, **2001**, *3*, 339.
[46] Bieche, I.; Onody, P.; Tozlu, S.; Driouch, K.; Vidaud, M.; Lidereau, R. *Int. J. Cancer*, **2003**, *106*, 758.
[47] Pollack, S.; Bruce, P.; Borenstein, M.; Lieberman, J. *Psychopharmacol. Bull*., **1994**, *30*, 227.

Received: 15 May, 2007 **Revised: 14 December, 2007** **Accepted: 14 December, 2007**